

# N-Heterocyclic Carbenes–Borane Complexes: A New Class of Initiators for Radical Photopolymerization

Mohamad-Ali Tehfe,<sup>†</sup> Malika Makhoul Brahmi,<sup>‡</sup> Jean-Pierre Fouassier,<sup>†</sup> Dennis P. Curran,<sup>\*,§</sup> Max Malacria,<sup>‡</sup> Louis Fensterbank,<sup>‡</sup> Emmanuel Lacôte,<sup>\*,‡</sup> and Jacques Lalevée<sup>\*,†</sup>

<sup>†</sup>Department of Photochemistry, CNRS, University of Haute Alsace, ENSCMu, 3 rue Alfred Werner, 68093 Mulhouse Cedex, France, <sup>‡</sup>UPMC Univ Paris 06, Institut Parisien de chimie moléculaire (UMR CNRS 7201), C. 229, 4 place Jussieu, 75005 Paris, France, and <sup>§</sup>Department of Chemistry, University of Pittsburgh, Pittsburgh, Pennsylvania 15260

Received November 11, 2009; Revised Manuscript Received January 14, 2010

**ABSTRACT:** Newly discovered N-heterocyclic carbene-boryl radicals (NHC-BH<sub>2</sub>•) derived from readily available N-heterocyclic carbene–boranes are found to be efficient initiators for acrylate photopolymerization. Laser flash photolysis (LFP) experiments were used to generate three carbene-boryl radicals, which were characterized by their transient absorption spectra with the aid of DFT calculations. Rate constants were measured for the generation of the carbene-boryl radicals by hydrogen abstraction with *tert*-butoxyl radical, a ketophosphonyl radical, and triplet benzophenone. Rate constants were also measured for the reactions of the carbene-boryl radicals with oxygen, three alkenes, two alkyl chlorides, and diphenyliodonium hexafluorophosphate. The observed trends were interpreted with the aid of measured oxidation potentials of the carbene–boranes and calculated ionization potentials of the carbene-boryls. N-Heterocyclic carbene–boranes show excellent potential as both photopolymerization co-initiators and mediators of small molecule radical reactions, and these results will help guide further development in both fields.

## Introduction

Radiation curing is often used to prepare coatings and other high-performance polymeric materials, and free radical photopolymerization with UV light has become one of the most important curing methods. Such photopolymerization processes are subject to strict spatial control and can easily be turned on or off at will. In addition, most industrial photopolymerization processes operate without solvents and thus meet the demands of green chemistry.<sup>1,2</sup>

UV-initiated photopolymerizations require a polymerization-initiating radical that can be generated in one of two ways. In monocomponent photoinitiating systems (called type I), homolytic single bond cleavage directly generates a pair of initiating radicals. In bicomponent photoinitiating systems (called type II), a hydrogen abstraction reaction of an excited state of the photoinitiator (\*PI) from a hydrogen donor (D–H) (called the co-initiator) generates the initiating radical (\*PI + D–H → PIH• + D•).<sup>1,2</sup> Bicomponent initiating systems are especially versatile, so the quest for new and more efficient co-initiators remains a crucial challenge for polymer synthesis. Existing photoinitiation systems are mainly based on aminoalkyl, benzoyl, or phosphinoyl radicals.<sup>1–3</sup> New initiating radicals with different geometries and properties and/or enhanced reactivity might provide new opportunities for polymer synthesis.<sup>4</sup> This could result in improved or altered properties of a final polymer, such as higher hardness or the introduction of hydrophobic surface properties.<sup>4,5</sup>

New multicomponent photoinitiating systems that generate silyl, germyl, and boryl radicals have been introduced by some of us.<sup>4–7</sup> In particular, ligand-complexed (ligated) boranes (L–BH<sub>3</sub>, where L is an amine<sup>8</sup> or a phosphine<sup>9</sup>) are good co-initiators. On photolysis with a suitable photoinitiator like

benzophenone, such ligated boranes produce amine-boryl initiating radicals (L–BH<sub>2</sub>•).

Complexes of N-heterocyclic carbene and boranes (NHC–boranes<sup>10</sup>) are a new family of ligated boranes that have recently been used in radical reductions of xanthates and related derivatives.<sup>11</sup> These reactions proceed through the intermediacy of a new class of boron-centered radicals, namely NHC-boryl radicals (NHC–BH<sub>2</sub>•).<sup>12</sup>

The early results with NHC-boryl radicals suggest that they may be very different from amine-boryl radicals. Amine-boranes have relatively strong B–H bonds (for Et<sub>3</sub>N·BH<sub>3</sub>, the bond dissociation energy is 101 kcal/mol),<sup>7b,13</sup> and the derived amine-boryl radicals are bent  $\sigma$  radicals with a high spin density on boron.<sup>11b,14</sup> These are radicals nucleophilic and function as polarity reversal catalysts in suitable settings.<sup>8j,15</sup>

In contrast, NHC-boranes have weaker C–H bonds (around 88 kcal/mol),<sup>12</sup> so they serve as radical hydrogen atom donors in Barton–McCombie reactions.<sup>11</sup> Because of the empty  $\pi$ -orbital on the central carbene carbon atom of NHC-boryl radicals, there is significant spin delocalization from the boron atom into the NHC ligand.<sup>12</sup> Accordingly, such radicals are planar,  $\pi$ -type radicals, not unlike the benzyl radical.

These marked differences led us to speculate that NHC-boranes might be better co-initiators for radical photopolymerization than amine-boranes. Moreover, the initiation ability of NHC-boryl radicals could be tuned by changing the NHC substituents. This is an attractive proposition because many NHC's are known<sup>16</sup> and because simple ligation with BH<sub>3</sub> generally produces the derived NHC-borane.

We report herein that NHC-boranes are efficient co-initiators for the polymerization of trimethylolpropane triacrylate (TMPTA). We use laser flash photolysis experiments for the first time to generate NHC-boryl radicals. Analysis of the time dependence of the spectra provided rate constants for formation

\*To whom correspondence should be addressed.

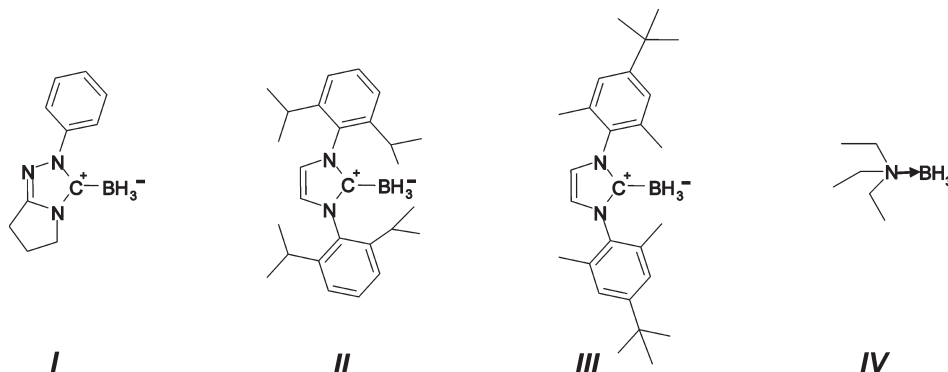


**Figure 1.** Investigated compounds.

of NHC-boryl radicals and for their onward reactions with alkenes, oxygen, alkyl chlorides, and diphenyliodonium hexafluorophosphate. The implications of these observations in both polymer chemistry and small molecule chemistry are discussed.<sup>17</sup>

Figure 1 shows the borane complexes that have been investigated. We selected three representative NHC-boranes: one in the triazolylidene series (2-phenyl-1,2,4-triazol-3-ylidene borane, **I**) and two in the diarylimidazolylidene series [1,3-bis(2,6-diisopropylphenyl)imidazol-2-ylidene borane (**II**), and 1,3-bis(2,6-dimethyl-4-*tert*-butylphenyl)imidazol-2-ylidene borane (**III**)]. These were selected to probe different electronic features (**I** vs **II–III**) and degrees of steric hindrance. Triethylamine–borane (**IV**) was selected as a control to compare the NHC-borane reactivity to typical amine–borane.<sup>7b</sup>

## Experimental Section and Methodology

**i. Investigated Compounds.** The borane complexes were prepared by following established procedures.<sup>11,12</sup> Triethylamine–borane (**IV**) was obtained from Aldrich. The model photoinitiator benzophenone (BP) was obtained from Aldrich. Ethyl dimethylaminobenzoate (EDB; Esacure EDB from Lamberti) was chosen as a reference amine co-initiator. Phenyl-bis(2,4,6-trimethylbenzoyl)phosphine oxide (BAPO) was obtained from Ciba (Basel, Switzerland). Methyl acrylate (MA), styrene (ST), ethyl vinyl ether (EVE), and diphenyliodonium hexafluorophosphate ( $\text{Ph}_2\text{I}^+$ ) were obtained from Aldrich. These compounds were used as received for most experiments. However, alkene stabilizers were removed by column purification (Aldrich AL-154) before the LFP experiments.

**ii. Laser Flash Photolysis Experiments (LFP).** Nanosecond laser flash photolysis (LFP) experiments were carried out using a Q-switched nanosecond Nd/YAG laser ( $\lambda_{\text{exc}} = 355 \text{ nm}$ , 9 ns pulses; energy reduced down to 10 mJ, from Powerlite 9010 Continuum) and an analyzing system consisting of a pulsed xenon lamp, a monochromator, a fast photomultiplier, and a transient digitizer.<sup>18</sup> The ketyl radical quantum yield ( $\Phi_K$ ) in the  $^3\text{BP}$ /borane complexes reaction was determined by a classical procedure.<sup>18,19</sup> The *t*-BuO $\cdot$  radicals were generated at 355 nm by the direct cleavage of di-*tert*-butyl peroxide.<sup>7a,18b</sup>

**iii. Redox Potentials.** The redox potentials were measured in acetonitrile by cyclic voltammetry with tetrabutylammonium hexafluorophosphate 0.1 M as a supporting electrolyte (Voltalab 06 radiometer).<sup>7a</sup> The working electrode was a platinum disk and the saturated calomel electrode (SCE) was used as the reference. The free energy changes for an electron transfer reaction between excited states and borane complexes ( $\Delta G_{\text{et}}$ ) were calculated from the classical Rehm–Weller equation (eq 1),<sup>20</sup> where  $E_{\text{ox}}$ ,  $E_{\text{red}}$ ,  $E_{\text{T}}$ , and  $C$  are respectively the oxidation potential of the donor, the reduction potential of the acceptor, the triplet state energy, and the Coulombic term for the initially

formed ion pair.  $C$  was neglected, as is customary done in polar solvents.<sup>7a</sup>

$$\Delta G_{\text{et}} = E_{\text{ox}} - E_{\text{red}} - E_{\text{T}} + C \quad (1)$$

**iv. DFT Calculations.** All the calculations were performed by using the hybrid functional B3LYP from the Gaussian 03 suite of program.<sup>21</sup> Reactants and products were fully optimized at the B3LYP/6-31+G\* level (checked for imaginary frequencies). The addition reaction enthalpy ( $\Delta H_{\text{r}}$ ) was calculated as the energy difference between the product and the reactants. Adiabatic ionization potentials (IP) for NHC-boryls were calculated from the energies of the relaxed neutral molecule and the corresponding relaxed ion at the B3LYP/6-31+G\* level.

The electronic absorption spectra were calculated with the time-dependent density functional theory at the MPW1PW91/6-31+G\* level on the relaxed geometry determined at the UB3LYP/6-31+G\* level.

**v. Photopolymerization Experiments.** For film polymerization experiments, a given PI was dissolved into a bulk formulation based on trimethylolpropane triacrylate (TMPTA from Cytec).<sup>22</sup> The laminated films (20  $\mu\text{m}$  thick) were deposited on a BaF<sub>2</sub> pellet and irradiated with polychromatic light (Xe–Hg lamp, Hamamatsu, L8252, 150 W). The evolution of the double bond content was followed by real-time FTIR spectroscopy (Nexus 870, Nicolet) at room temperature (RT).<sup>22</sup>

## Results and Discussion

**a. Photopolymerization of TMPTA with NHC-Borane Co-initiators.** The polymerization kinetics of trimethylolpropane triacrylate (TMPTA) were examined by measuring the consumption of monomer in experiments with benzophenone as the photoinitiator in both the absence and presence of NHC-borane co-initiators. Figure 2A shows the percent conversion of TMPTA as a function of time, with the reference EDB (a), Et<sub>3</sub>N–BH<sub>3</sub> (c), the three NHC-boranes (b, d, e), and without co-initiator (f).

The photopolymerization can be induced by BP alone, but this process is not very efficient (Figure 2A, curve f).<sup>23</sup> This initiation background is ascribed to abstraction of a labile hydrogen atom from the monomer (TMPTA) by the benzophenone triplet state ( $^3\text{BP}$ ). In contrast, addition of the NHC-borane co-initiators **I–III** (1% w/w) significantly improved the rate of polymerization (Figure 2A, curves b, d, e). This suggests that NHC-boryl radicals were generated by hydrogen abstraction by  $^3\text{BP}$  and in turn that these radicals initiated the polymerization (see below for mechanistic details).

The most promising co-initiator is **I** (curve b), with a polymerization rate close to that of the reference co-initiator ethyl-dimethylaminobenzoate (EDB) (curve a).<sup>1,2</sup> However,

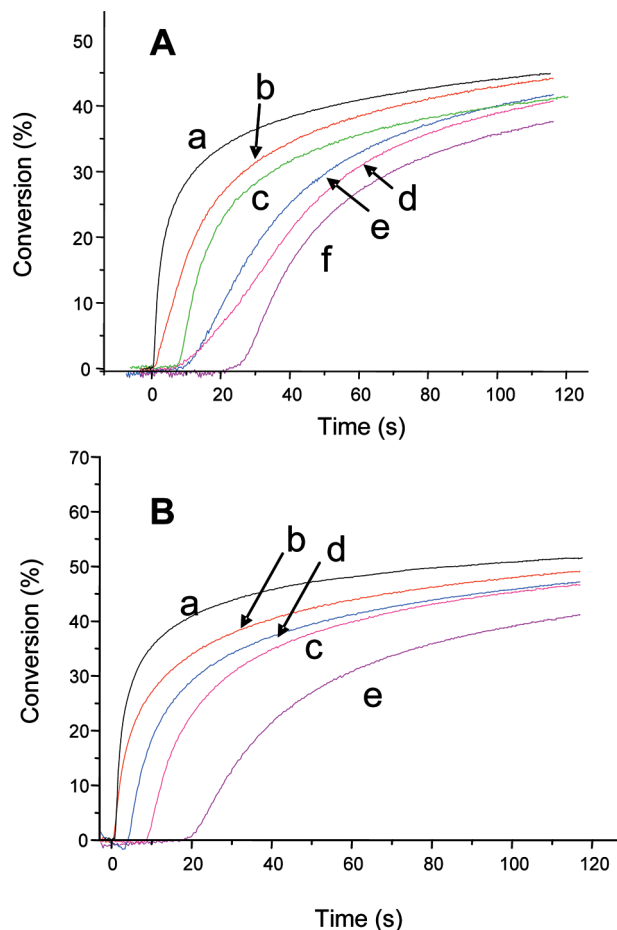


**Figure 2.** (A) Radical photopolymerization ability of various BP/co-initiator couples (1%/1% w/w; in TMPTA, in laminate): EDB (a); I (b); IV (c); II (d); III (e); without co-initiator (f). (B) Radical photopolymerization ability of various BP/co-initiator couples (1%/1% w/w; in TMPTA, in laminate): EDB (a); I (b); II (c); III (d); without co-initiator (e) with Ph<sub>2</sub>I<sup>+</sup> as additive (1% w/w).

complex I triggered a more rapid polymerization than amine-borane IV (Figure 2A, compare curve b to curve c). At  $t = 10$  s, the conversion was 20% for BP/I but only 5% for BP/IV.

Diphenyliodonium hexafluorophosphate (Ph<sub>2</sub>I<sup>+</sup>PF<sub>6</sub><sup>−</sup>) is a popular additive in multicomponent initiation systems,<sup>1,2</sup> and the conversion of TMPTA as a function of time in the presence of Ph<sub>2</sub>I<sup>+</sup>PF<sub>6</sub><sup>−</sup> is shown in Figure 2B. Indeed, the polymerization rate was strongly increased for all the NHC-boranes relative to the control without co-initiator (curve e). Again, the polymerization rate for BP/I/Ph<sub>2</sub>I<sup>+</sup>PF<sub>6</sub><sup>−</sup> is quite similar to that of the classical system BP/EDB/Ph<sub>2</sub>I<sup>+</sup>PF<sub>6</sub><sup>−</sup> (compare curves a and b).

Unfortunately, existing amine/iodonium salt formulations are unstable because these two reagents react directly at the temperature used for polymerization (RT).<sup>22c,24</sup> For example the BP/EDB/Ph<sub>2</sub>I<sup>+</sup>PF<sub>6</sub><sup>−</sup> formulation cannot be stored without decomposition and must be freshly prepared. In contrast, a photoinitiator formulation including the BP/I/Ph<sub>2</sub>I<sup>+</sup>PF<sub>6</sub><sup>−</sup> was stable for at least 1 week at RT. This stability of the NHC-BH<sub>3</sub>/Ph<sub>2</sub>I<sup>+</sup>PF<sub>6</sub><sup>−</sup> combination is a significant advantage for practical applications.

To understand how the NHC-boryl radical initiates polymerization and to learn about the effects of the carbene substituent, we examined in detail the kinetics of both the formation of the boryl radical and its reactions with several key small molecules.

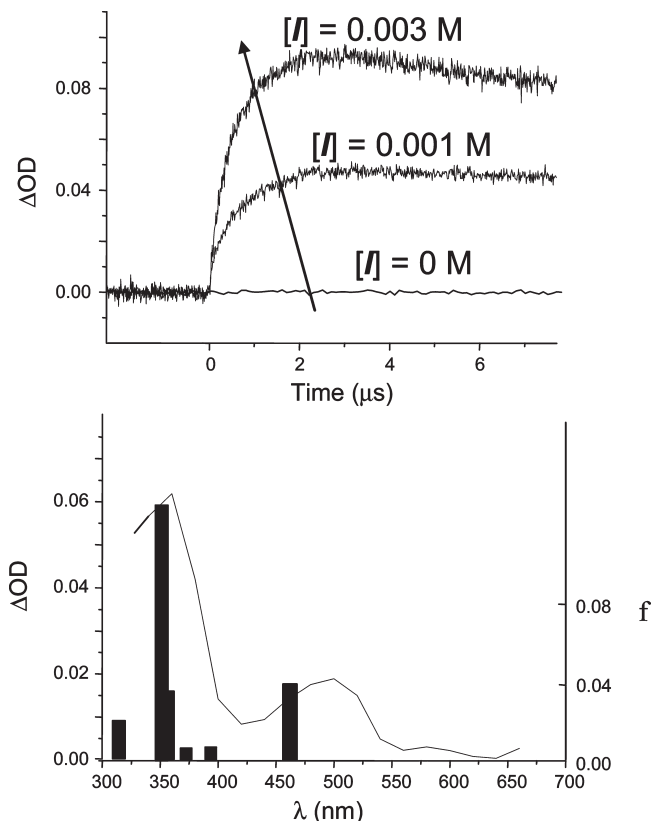
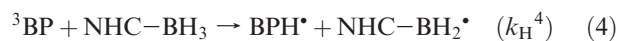
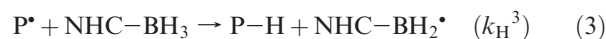
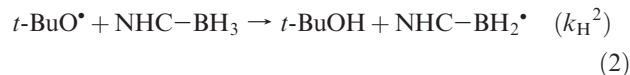


**Figure 3.** (A) Kinetics for the formation of I• at  $\lambda = 485$  nm in acetonitrile/di-*tert*-butyl peroxide; the I concentrations are indicated. (B) Transient absorption spectrum in acetonitrile/di-*tert*-butyl peroxide at  $t = 0.5 \mu\text{s}$ . The rise of the NHC-boryl radical occurs within 500 ns.

#### b. Formation and Reactivity of the NHC-Boryl Radicals.

We used three different approaches to form NHC-boryl radicals based on hydrogen abstraction reactions by (1) the *tert*-butoxyl radical (*t*-BuO•) (eq 2), (2) Turro's ketophosphinoyl radical (MesC(=O)Ph(O=)P•, or P• for short (eq 3),<sup>3</sup> and (3) the benzophenone triplet state (<sup>3</sup>BP, eq 4). *t*-BuO• and P• were generated by the direct cleavage of di-*tert*-butyl peroxide or BAPO at 355 nm.<sup>1b,18b</sup> The triplet state of BP was obtained by irradiation at 355 nm (quantum yield of 1.0).<sup>19</sup>



The NHC-boryl radicals I•–IV• generated by LFP of I–IV from reaction 2 gave intense absorption in the UV spectrum of > 300 nm. The transient absorption spectra of I•, II•, and III• recorded by laser flash photolysis are shown in Figures 3B, 4A, and 4B, respectively. The spectrum of IV• is known.<sup>7b,17a</sup>

The LFP spectrum of I• spreads over the visible range with a maximum absorption at about 500 nm. The absorptions of II• and III• are blue-shifted ( $\lambda_{\text{max}} \sim 350$  nm), and, like their structures, their spectra are quite similar. The spectral features predicted by time-dependent density functional theory modeling (TD-DFT) fit the experimental data quite well.<sup>25</sup> The transitions calculated for I• (456 and 354 nm) are in good

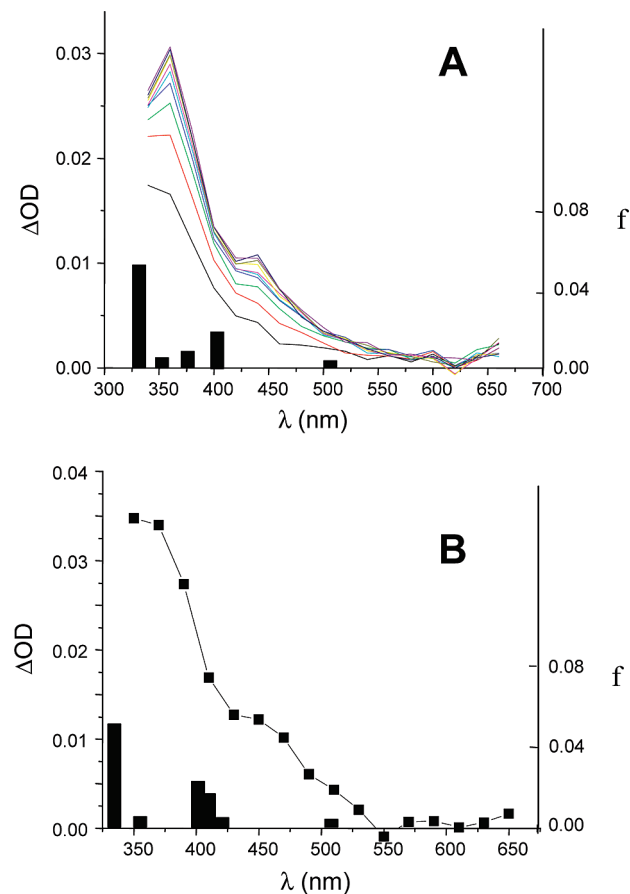


**Figure 4.** Transient absorption spectra in acetonitrile/di-*tert*-butylperoxide of (A) **II\*** (recorded at different times after the laser excitation (from 0.5 to 14  $\mu$ s by steps of 0.85  $\mu$ s). The rise of the boryl radical occurs within 500 ns. (B) **III\*** at  $t = 0.5 \mu$ s. The rise of the boryl radical occurs within 500 ns. The calculated absorption spectra are also given (Sticks) together with the oscillator strength ( $f$ ).

**Table 1.** Rate Constants ( $k_H^2$ ,  $k_H^3$ ,  $k_H^4$ ) for the Formation of the NHC-Boryl Radicals

	$k_H^2(t\text{-BuO}^\bullet)/10^7 \text{ M}^{-1} \text{ s}^{-1}$	$k_H^3(\text{P}^\bullet)/10^7 \text{ M}^{-1} \text{ s}^{-1}$	$k_H^4(^3\text{BP})/10^7 \text{ M}^{-1} \text{ s}^{-1}$
<b>I</b>	15	n.d. <sup>a</sup>	55 (0.90) <sup>b</sup>
<b>II</b>	9.5	n.d.	28 (0.25)
<b>III</b>	12	4.1	39 (0.55)
<b>IV</b>	5.9 (5.3) <sup>c</sup>	< 0.05	9.1 (0.73)

<sup>a</sup> n.d.: not determined. <sup>b</sup> Ketyl radical quantum yield ( $\Phi_K$ ). <sup>c</sup> From ref 17a.

agreement with the experimental ones ( $\sim 500$  and  $350$  nm), and their relative intensities are well reproduced. For **II\*** and **III\***, a similar good agreement was found (calcd  $\sim 330$  nm; experimental  $\sim 350$  nm).

Rate constants for hydrogen abstraction were measured by conducting time-dependent LFP experiments. For example, assessment of the rising time of the transient of **I\*** at  $475$  nm (Figure 3A) provided the rate constant  $k_H^2$  for the reaction of **I** with  $t\text{-BuO}^\bullet$  (eq 2). For eqs 3 and 4,  $k_H^3$  and  $k_H^4$  values were extracted from the decay times of **P\*** and  $^3\text{BP}$  observed at  $450$  and  $525$  nm, respectively (Figure 5). These rate constants for hydrogen abstraction reactions of complexes **I–IV** are gathered in Table 1. For the reactions benzophenone, eq 4, we also measured the ketyl radical quantum yields in the usual way, and these values are in parentheses in Table 1. In complementary work, rate constants  $k_H$  for eq 2 have recently been measured by kinetic

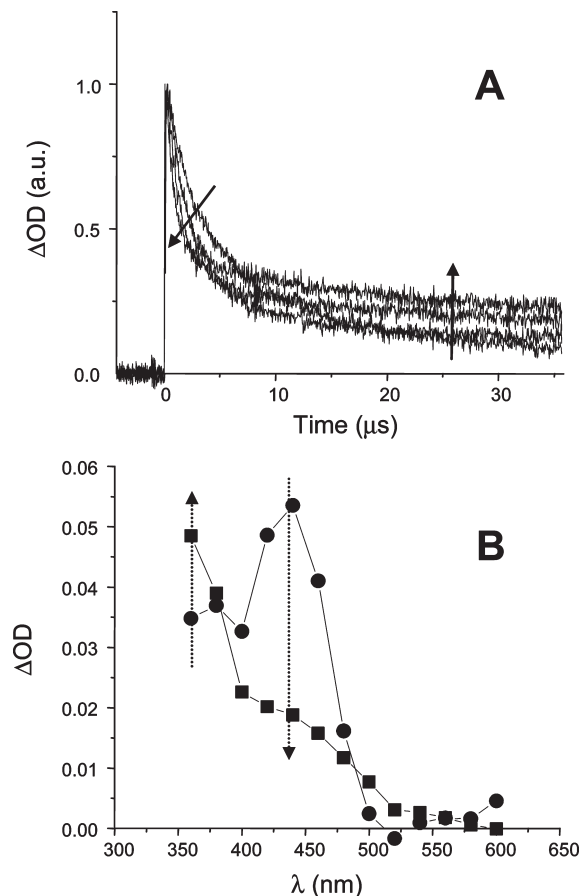


**Figure 5.** (A) Kinetics at  $450$  nm for the interaction of the phosphinoyl radical **P\*** with **III**. (B) Transient absorption spectra in acetonitrile at  $t = 0.0 \mu$ s (circle) corresponding to **P\*** and  $t = 20.0 \mu$ s (square) corresponding to **III\***.

EPR spectroscopy,<sup>12b</sup> and these values are in good agreement with the LFP numbers.

High rate constants were obtained for the formation of all the NHC-boryl radicals in reactions with  $t\text{-BuO}^\bullet$  (eq 2) and  $^3\text{BP}$  (eq 4) ( $k_H^2$  and  $k_H^4 > 10^7 \text{ M}^{-1} \text{ s}^{-1}$ ) (Table 1). In principle, these reactions may occur either by direct hydrogen atom transfer or by electron transfer followed by proton transfer. To address this point, we measured the oxidation potentials for **III** ( $> 1.5$  V) and **IV** ( $1.5$  V) by cyclic voltammetry, as described in the Experimental Section. By using a reduction potential of  $-1.79$  V and a triplet state energy of  $2.98$  eV for **BP**,<sup>19</sup> we estimate that electron transfer reactions of **III** and **IV** to  $^3\text{BP}$  are endergonic ( $\Delta G_{\text{et}}$  higher than  $+0.31$  eV is expected from eq 1). This suggests that the reaction in eq 4 with **III** (or **IV**) probably does not correspond to an electron/proton transfer sequence, but to a pure hydrogen atom transfer with the triplet state of benzophenone reacting like an alkoxy radical.

The trend observed for  $k_H^2$  and  $k_H^4$  was **IV** < **II** < **III** < **I**. A similar behavior was also found for reaction 3, this time with **IV**  $\ll$  **III**. Clearly, NHC-boranes **I**, **II**, and **III** are better H atom donors toward oxygen or phosphorus-centered radicals than the reference amine–borane **IV**. This trend parallels the respective bond dissociation energies [BDE(B–H)]. Complexes **I** and **IV** have calculated BDEs of  $79$  kcal/mol<sup>11</sup> and  $101$  kcal/mol,<sup>7b</sup> respectively, while that of **II** has been determined experimentally at  $88$  kcal/mol.<sup>12a</sup> This latter value is considerably higher than the calculated value ( $80$  kcal/mol<sup>11</sup>). Nonetheless, by any measure,



**Table 2.** Interaction Rate Constants of the NHC-Boryl Radicals with Various Additives at RT in Acetonitrile/*Di-tert*-butyl Peroxide Solvent<sup>a</sup>

	$k'_{\text{add}}(\text{R}^{\bullet}/\text{O}_2)/10^8$ $\text{M}^{-1} \text{s}^{-1}$	$k_{\text{add}}(\text{R}^{\bullet}/\text{MA})/10^6$ $\text{M}^{-1} \text{s}^{-1}$	$k_{\text{add}}(\text{R}^{\bullet}/\text{STY})/10^5$ $\text{M}^{-1} \text{s}^{-1}$	$k_{\text{add}}(\text{R}^{\bullet}/\text{EVE})/10^5$ $\text{M}^{-1} \text{s}^{-1}$	$k_{\text{Cl}}(\text{R}^{\bullet}/\text{CCl}_4)/10^7$ $\text{M}^{-1} \text{s}^{-1}$	$k_{\text{Cl}}(\text{R}^{\bullet}/\text{CH}_2\text{Cl}_2)/10^5$ $\text{M}^{-1} \text{s}^{-1}$	$k_{\text{ox}}(\text{R}^{\bullet}/\text{Ph}_2\text{I}^+)/10^9$ $\text{M}^{-1} \text{s}^{-1}$
<b>I</b> <sup>•</sup>	> 2	6.0	5.9	< 2	11	< 3	0.6 (5.57) <sup>c</sup>
<b>II</b> <sup>•</sup>	> 2	0.08	< 3	< 2	2	< 3	n.d. (4.96)
<b>III</b> <sup>•</sup>	> 2	0.52	n.d. <sup>b</sup>	n.d.	49	< 5	0.6 (4.96)
<b>IV</b> <sup>•</sup>	> 7	130 (540)	3200	< 1	440	1200	2.4 (4.7)

<sup>a</sup> MA, STY, and EVE stand for methylacrylate, styrene, and ethyl vinyl ether. <sup>b</sup> n.d.: not determined. <sup>c</sup> Ionization potential at the UB3LYP/6-31+G\* level in eV. <sup>d</sup> Taken from ref 17a.

the carbene–boranes have weaker B–H bonds than the amine–borane.

The good hydrogen-donating property of N-heterocyclic carbene–borane complexes is also in agreement with their fairly high rate constant of reaction with secondary carbon-centered radicals ( $k = 4 \times 10^4 \text{ M}^{-1} \text{ s}^{-1}$  for **II**).<sup>12a</sup> We believe that this donation ability contributes to the better initiation by NHC-boranes compared to the amine–borane.

The ketyl radical quantum yields ( $\Phi_K$ ) for reaction 4—which are equal to the boryl radical quantum yields—are also reported in Table 1. These quantum yields strongly decrease in the order **I** (0.90) > **III** (0.55) > **II** (0.25). Because <sup>3</sup>BP is quite bulky, the lowering of  $\Phi_K$  throughout the series can probably be ascribed to the steric hindrance associated with the NHC complex. Complex **II** exhibits a higher hindrance than **III** due to its diisopropylphenyl groups. In turn, the *o,o'*-dimethylphenyl groups on **III** are more demanding than the nitrogen substituents in **I**. Still, one must exercise caution when comparing **I** to **II** or **III** because electronic effects may also play a role. These preliminary results suggest that steric shielding about the reactive B–H bond by the NHC substituents<sup>26</sup> can be used to fine-tune the reactivity of both the NHC-borane and the associated NHC-boryl radical.

**Addition of NHC-Boryl Radicals onto Double Bonds.** The direct observation of NHC-boryl radicals offered by time-resolved LFP allowed us to measure their absolute reaction rate constants in several important radical/molecule and radical/ion reactions involved in polymerizations and other settings. All the rate constants measured by these experiments are compiled in Table 2. Initial experiments showed that the ligated boryl radicals react very rapidly with oxygen ( $k_{\text{O}_2} > 2 \times 10^8 \text{ M}^{-1} \text{ s}^{-1}$ , Table 2), so the subsequent kinetic experiments with other molecules were all carried out under argon.

The results of several typical experiments to measure boryl radical rate constants are summarized in Figure 6. Figure 6A shows how the lifetime of **III**<sup>•</sup> decreases with increasing concentration of methyl methacrylate (MA), while Figure 6B shows the results with **III**<sup>•</sup> and CCl<sub>4</sub>. Similar experiments were conducted with the other radicals **I**<sup>•</sup>, **II**<sup>•</sup>, and **IV**<sup>•</sup> and with ethyl vinyl ether (EVE), dichloromethane (CH<sub>2</sub>Cl<sub>2</sub>), and diphenyliodonium (Ph<sub>2</sub>I<sup>+</sup>). The data were processed in the usual way to provide the rate constants in Table 2.

The addition rate constants ( $k_{\text{add}}$ ) onto methyl acrylate (MA), styrene (STY), and ethyl vinyl ether (EVE) are gathered in columns 2–4 of Table 2. For the addition onto the electron deficient alkene (MA), the reactivity decreases in the order **IV**<sup>•</sup> > **I**<sup>•</sup> > **III**<sup>•</sup> > **II**<sup>•</sup>. The rate constants span over 3 orders of magnitude ( $1.3 \times 10^8$  and  $8 \times 10^4 \text{ M}^{-1} \text{ s}^{-1}$  for **IV**<sup>•</sup> and **II**<sup>•</sup>, respectively). A similar trend was found for the addition onto styrene ( $k_{\text{add}}$  of  $3.2 \times 10^8$ ,  $5.9 \times 10^5$ , and  $< 3 \times 10^5 \text{ M}^{-1} \text{ s}^{-1}$  for **IV**<sup>•</sup>, **I**<sup>•</sup>, and **III**<sup>•</sup>, respectively).

For the addition onto the electron-rich alkene (EVE), the rate constants are below  $2 \times 10^5 \text{ M}^{-1} \text{ s}^{-1}$  for all radicals. The combination of fast addition to an electron-poor alkene and

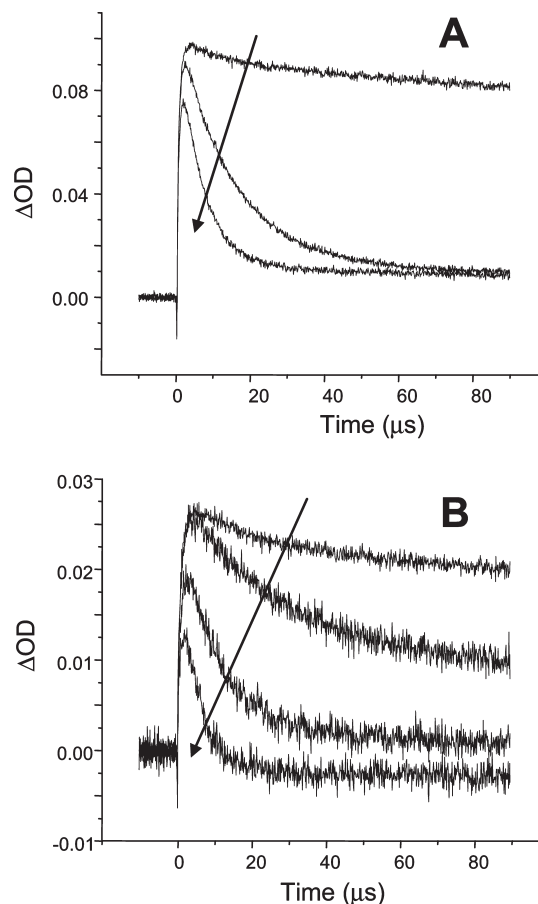


**Figure 6.** (A) Kinetics at 330 nm corresponding to **III**<sup>•</sup> for different MA concentrations from [MA] = 0 M to [MA] = 0.23 M. (B) Kinetics at 330 nm corresponding to **III**<sup>•</sup> for different CCl<sub>4</sub> concentrations from [CCl<sub>4</sub>] = 0 M to [CCl<sub>4</sub>] =  $4.6 \times 10^{-4}$  M.

slow addition to an electron-rich alkene suggests that NHC-boryl radicals may be nucleophilic.

The amine-boryl radical **IV**<sup>•</sup> reacts much more rapidly with MA and STY than the three carbene-boryl radicals. The lower stabilization of **IV**<sup>•</sup> [as reflected by higher BDE(B–H)] may explain this higher reactivity. As mentioned earlier, amine-boryl radicals are pyramidal  $\sigma$ -type radicals.<sup>8a,12</sup> In contrast, ESR spectroscopy showed that NHC-boryl is a planar structure at boron, with a  $\pi$ -type radical similar to a benzyl radical.<sup>12</sup> The unpaired electron is delocalized into the NHC ring. DFT modeling of the radicals supports this picture, and the SOMOs of **I**<sup>•</sup>–**III**<sup>•</sup> are shown in Figure 7. The spin densities at boron were calculated at 0.46, 0.48, and 0.42 for **I**<sup>•</sup>, **III**<sup>•</sup>, and **II**<sup>•</sup>, while the spin density for **IV**<sup>•</sup> was 1.04.<sup>27</sup>

The higher  $k_{\text{add}}$  for Et<sub>3</sub>N–BH<sub>2</sub><sup>•</sup> compared to NHC-boryl radicals can also be understood by the calculated reaction exothermicity for the addition onto MA (–30 and –16 kJ/mol for **I**<sup>•</sup> and **II**<sup>•</sup> vs –146 kJ/mol for **IV**<sup>•</sup> at the UB3LYP/6-31+G\* level).

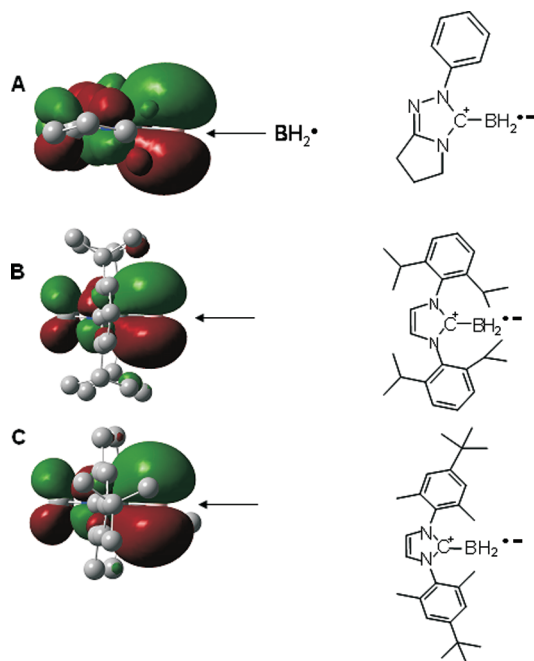


**Figure 7.** Singly occupied molecular orbitals (SOMOs) (isovalue 0.02) for (A) **I**<sup>•</sup>, (B) **II**<sup>•</sup>, and (C) **III**<sup>•</sup> (the hydrogens are not depicted). The radical center is indicated by an arrow.

Steric hindrance was again expected to play a role in the addition rate of **I**<sup>•</sup>–**III**<sup>•</sup> onto olefins. While the boron spin densities of these radicals and the exothermicities of their alkene addition reactions are in the same range (see above),  $k_{\text{add}}$  spans over 2 orders of magnitude for MA, from  $6 \times 10^6 \text{ M}^{-1} \text{ s}^{-1}$  for **I**<sup>•</sup> down to  $0.08 \times 10^6 \text{ M}^{-1} \text{ s}^{-1}$  for **II**<sup>•</sup>. This reflects the decrease in steric hindrance at the reaction center in the series **II**<sup>•</sup> > **III**<sup>•</sup> > **I**<sup>•</sup>. Figure 7 shows how the aryl substituents in **II** shield the SOMO and thus prevent efficient overlap with the  $\pi$  orbital of the olefin. This shielding is less marked in **III** than **II** and not observed for **I**.

**Reactivity of NHC-Boryl Radicals toward Alkyl Halides.** The reactions of NHC-boryl radicals with alkyl halides are potentially important elementary steps in small molecule radical chemistry with NHC-boranes as mediators.<sup>17a</sup> The rate constants ( $k_{\text{Cl}}$ ) for reactions of **I**–**IV** with  $\text{CCl}_4$  and  $\text{CH}_2\text{Cl}_2$  are gathered in columns 5 and 6 of Table 2.

The reactivity with  $\text{CCl}_4$  decreased in the order **IV**<sup>•</sup> > **III**<sup>•</sup> > **I**<sup>•</sup> > **II**<sup>•</sup>, and the variation of  $k_{\text{Cl}}$  was large ( $2\text{--}440 \times 10^7 \text{ M}^{-1} \text{ s}^{-1}$ ). Surprisingly though, **III**<sup>•</sup> reacts about 5 times faster with  $\text{CCl}_4$  than **I**<sup>•</sup>, even though **III**<sup>•</sup> is more sterically hindered (see below). Only **IV**<sup>•</sup> reacts with  $\text{CH}_2\text{Cl}_2$  with a significant rate constant ( $k_{\text{Cl}} > 10^5 \text{ M}^{-1} \text{ s}^{-1}$ , Table 2); none of the NHC-boryls reacted fast enough for  $k_{\text{Cl}}$  to be measured by using the LFP setup ( $k_{\text{Cl}} < 10^5 \text{ M}^{-1} \text{ s}^{-1}$ ).

The high reactivity of **IV**<sup>•</sup> toward both  $\text{CCl}_4$  and  $\text{CH}_2\text{Cl}_2$  is consistent with the prior addition results. Again, some steric hindrance is at least partly responsible for the change in  $k_{\text{Cl}}$  ( $\text{CCl}_4$ ) between **II**<sup>•</sup> and **III**<sup>•</sup>. However, NHC-boryl radicals have low ionization potentials (Table 2), so other factors may also be in play. Indeed, the charge transfer from NHC-boryl radicals to  $\text{CCl}_4$  might explain in part their much higher reactivity toward  $\text{CCl}_4$ , compared to  $\text{CH}_2\text{Cl}_2$ . That **III**<sup>•</sup> is more reactive than **I**<sup>•</sup> toward  $\text{CCl}_4$  can be ascribed to a lower oxidation potential for **III**<sup>•</sup> (4.96 eV vs 5.57 eV, Table 2), leading to increased polar effects for this radical.

**Oxidation of NHC-Boryl Radicals to NHC-Borenium Cations with  $\text{Ph}_2\text{I}^+\text{PF}_6^-$ .** Iodonium salts have low reduction potentials (ca.  $-0.2 \text{ V}$ ). Thus, diphenyliodonium

hexafluorophosphate is often used to oxidize radicals.<sup>28</sup> The rate constants for the chemical oxidation of NHC-boryl radicals with  $\text{Ph}_2\text{I}^+\text{PF}_6^-$  were very high, approaching the diffusion limit ( $k > 10^8 \text{ M}^{-1} \text{ s}^{-1}$ , Table 2, column 7). Presumably NHC-borenium cations ( $\text{NHC-BH}_2^+$ ) are the immediate products of these reactions.

To help understand these reactions, we calculated the ionization potentials (IP) for radicals **I**<sup>•</sup>–**IV**<sup>•</sup> at the UB3LYP/6-31+G\* level. The IPs are listed in parentheses in the last column of Table 2. The values are very low (4.9–5.6 eV), further hinting at an oxidation of the radicals to the presumed complexed borenium cations. The low values also fit with the nucleophilic character of NHC-boryl radicals, as evidenced by the addition onto electron-poor but not electron-rich double bonds. Aminoalkyl radicals, which exhibit similar ionization potentials,<sup>29</sup> are also oxidized at near-diffusion-controlled rates, in agreement with the postulated oxidation to borenium cations.

Gabbai reported the reduction potential of borenium cation ([1,3-dimethylimidazol-2-ylideneBMe<sub>2</sub>]<sup>+</sup>OTf) to be  $-1.8 \text{ V}$  (vs Fc/Fc<sup>+</sup>).<sup>10j</sup> The reduction of the borenium led to a NHC-boryl radical, which was characterized by ESR spectroscopy. Though Gabbai's NHC-borane has substituents on boron and ours do not, Gabbai's negative reduction potential is in line with the high rate constants for oxidation found reported herein.

**c. Mechanism of Initiation of Polymerization.** The polymerization rates observed with NHC-borane co-initiators (Figure 2) (**I** > **III** > **II**) are in good agreement with the measured reactivity of the NHC-boryl radicals (Table 2). Both the NHC-boryl radical quantum yields (for the <sup>3</sup>BP/NHC-borane hydrogen abstraction reaction) and the rate constant ( $k_{\text{add}}$ ) for addition of NHC-boryl radical onto acrylate decrease in the same order. A competitive deactivation pathway of <sup>3</sup>BP by the monomer due to physical quenching also exists.<sup>30</sup> However, this affects in the same extent all the NHC-borane complexes considered.<sup>23</sup>

For the photoinitiating systems BP/NHC–BH<sub>3</sub>/Ph<sub>2</sub>I<sup>+</sup>PF<sub>6</sub><sup>−</sup>, it was found that the polymerization rates are strongly increased by addition of Ph<sub>2</sub>I<sup>+</sup>PF<sub>6</sub><sup>−</sup>. We believe this stems from the high rate constants for the oxidation of boryl radicals to borenium cations (eq 5).



The rapid conversion of an NHC-boryl radical to a borenium simultaneously releases a phenyl radical (Ph<sup>•</sup>). Phenyl radicals have higher  $k_{\text{add}}$  (MA) [ $1.9 \times 10^8 \text{ M}^{-1} \text{ s}^{-1}$ ],<sup>31</sup> and thus they initiate the radical photopolymerization better than the NHC-boryl radicals. The reactivity trend (**I** > **III** > **II**) is in agreement with the radical quantum yields (for <sup>3</sup>BP/NHC–BH<sub>3</sub>) since the oxidation rate constants remain quite similar for **I**<sup>•</sup>–**III**<sup>•</sup>.

## Conclusions

NHC-boranes have been found to be an efficient new class of co-initiators for radical photopolymerization. The observation of the derived NHC-boryl radicals by LFP allowed us to determine the rate constants of the elementary events featured in the polymerization. This direct window on reactivity has shown that the properties of the complexes can be modulated by changing the carbene. This is important for polymerization because the great variety of existing N-heterocyclic carbenes may be parlayed into a family of initiators with a predictable range of properties. The present work focuses on gaining a better knowledge of the structure/activity relationship, with a view to introduce an

optimized co-initiator with better hydrogen-donating properties and rate constants of addition onto monomers.

## References and Notes

- (1) (a) Pappas, S. P. *UV Curing: Science and Technology*; Technologie Marketing Corporation: 1985; Vol. II. (b) Dietliker, K. *A Compilation of Photoinitiators Commercially Available for UV Today*; Sita Technology Ltd.: Edinburgh, London, 2002. (c) Neckers, D. C. *UV and EB at the Millennium*; Sita Technology: London, 1999. (d) Schwalm, R. *UV Coatings: Basics, Recent Developments and New Applications*; Elsevier: Oxford UK, 2007. (e) Davidson, R. S. *Exploring the Science, Technology and Applications of UV and EB Curing*; SITA Technology Ltd.: London, 1999. (f) Krongauz, V.; Trifunac, A. *Photoresponsive Polymers*; Chapman and Hall: New York, 1994. (g) Belfield, K.; Crivello, J. V. *Photoinitiated Polymerization*; ACS Symposium 847; American Chemical Society: Washington, DC, 2003.
- (2) (a) Fouassier, J. P. *Photoinitiation, Photopolymerization and Photocuring: Fundamental and Applications*; Hanser Publishers: New York, 1995. (b) *Photochemistry and UV Curing*; Fouassier, J. P., Ed.; Researchsignpost: Trivandrum, India, 2006.
- (3) (a) Sluggett, G. W.; McGarry, P. F.; Koptiyug, I. V.; Turro, N. J. *J. Am. Chem. Soc.* **1996**, *118*, 7367–7372. (b) Jockusch, S.; Landis, M. S.; Freiermuth, B.; Turro, N. J. *Macromolecules* **2001**, *34*, 1619–1626.
- (4) (a) Fedorov, A. V.; Ermoshkin, A. A.; Mejrinski, A.; Neckers, D. C. *Macromolecules* **2007**, *40*, 3554–3560. (b) Fedorov, A. V.; Ermoshkin, A. A.; Neckers, D. C. *J. Appl. Polym. Sci.* **2008**, *107*, 147–152. (c) Ganster, B.; Fischer, U. K.; Moszner, N.; Liska, R. *Macromol. Rapid Commun.* **2008**, *29*, 57–62. (d) Durmaz, Y. Y.; Moszner, N.; Yagci, Y. *Macromolecules* **2008**, *41*, 6714–6718. (e) Andrzejewska, E.; Zych-Tomkowiak, D.; Andrzejewski, M. *Macromolecules* **2006**, *39*, 3777–3785. (f) Cramer, N. B.; Scott, J. P.; Bowman, C. N. *Macromolecules* **2002**, *35*, 5361–5365. (g) Lee, T. Y.; Guymon, C. A.; Jonsson, E. S.; Hait, S.; Hoyle, C. N. *Macromolecules* **2005**, *38*, 7529–7531. (h) Lalevée, J.; El-Roz, M.; Allonas, X.; Fouassier, J. P. *Macromolecules* **2007**, *40*, 2003–2010.
- (5) Lalevée, J.; El-Roz, M.; Allonas, X.; Fouassier, J. P. *Prog. Org. Coat.* **2009**, *65*, 457–461.
- (6) (a) Lalevée, J.; El-Roz, M.; Allonas, X.; Fouassier, J. P. *Macromolecules* **2007**, *40*, 8527–8530. (b) Lalevée, J.; Dirani, A.; El-Roz, M.; Allonas, X.; Fouassier, J. P. *J. Polym. Sci., Part A: Polym. Chem.* **2008**, *46*, 3042–3047.
- (7) (a) Lalevée, J.; Tehfe, M. A.; Allonas, X.; Fouassier, J. P. *Macromolecules* **2008**, *41*, 9057–9062. (b) Lalevée, J.; Blanchard, N.; Chany, A.-C.; Tehfe, M. A.; Allonas, X.; Fouassier, J. P. *J. Phys. Org. Chem.* **2009**, *22*, 986–993.
- (8) (a) *Radicals in Organic Synthesis*, 1st ed.; Renaud, P.; Sibi, M. P., Eds.; Wiley-VCH: Weinheim, 2001. (b) Marti, V. P. J.; Roberts, B. P. *J. Chem. Soc., Perkin Trans. 2* **1986**, 1613–1621. (c) Baban, J. A.; Marti, V. P. J.; Roberts, B. P. *Tetrahedron Lett.* **1985**, *26*, 1349–1352. (d) Baban, J. A.; Marti, V. P. J.; Roberts, B. P. *J. Chem. Soc., Perkin Trans. 2* **1985**, 1723–1733. (e) Baban, J. A.; Roberts, B. P. *J. Chem. Soc., Chem. Commun.* **1983**, 1224–1226. (f) Johnson, K. M.; Kirwan, J. N.; Roberts, B. P. *J. Chem. Soc., Perkin Trans. 2* **1990**, 1125–1132. (g) Giles, J. R. M.; Roberts, B. P. *J. Chem. Soc., Perkin Trans. 2* **1982**, 743–755. (h) Baban, J. A.; Roberts, B. P. *J. Chem. Soc., Perkin Trans. 2* **1986**, 1607–1611. (i) Lucarini, M.; Pedulli, G. F.; Valgimigli, L. *J. Org. Chem.* **1996**, *61*, 4309–4313. (j) Roberts, B. P. *Chem. Soc. Rev.* **1999**, *28*, 25–35.
- (9) Barton, D. H. R.; Jacob, M. *Tetrahedron Lett.* **1998**, *39*, 1331–1334.
- (10) (a) Kuhn, N.; Henkel, G.; Kratz, T.; Kreutzberg; Boese, J. R.; Maulitz, A. H. *Chem. Ber.* **1993**, *126*, 2041–2045. (b) Wacker, A.; Pritzkow, H.; Siebert, W. *Eur. J. Inorg. Chem.* **1999**, 789–793. (c) Rammial, T.; Jong, H.; McKenzie, I. D.; Jennings, M.; Clyburne, J. A. C. *Chem. Commun.* **2003**, 1722–1723. (d) Yamaguchi, Y.; Kashiwabara, T.; Ogata, K.; Miura, Y.; Nakamura, Y.; Kobayashi, K.; Ito, T. *Chem. Commun.* **2004**, 2160–2161. (e) Wang, Y.; Quillian, B.; Wei, P.; Wannere, C. S.; Xie, Y.; King, R. B.; Schaefer, H. F. III; Schleyer, P. v. R.; Robinson, G. H. *J. Am. Chem. Soc.* **2007**, *129*, 12412–12413. (f) Holschumacher, D.; Bannenberg, T.; Hrib, C. G.; Jones, P. G.; Tamm, M. *Angew. Chem., Int. Ed.* **2008**, *47*, 7428–7432. (g) Chase, P. A.; Stephan, D. W. *Angew. Chem., Int. Ed.* **2008**, *47*, 7433–7437. (h) Lee, K. S.; Zhugralin, A. R.; Hoveyda, A. H. *J. Am. Chem. Soc.* **2009**, *131*, 7253–7255. (i) Wood, T. K.; Piers, W. E.; Keay, B. A.; Parvez, M. *Angew. Chem., Int. Ed.* **2009**, *48*, 4009–4012. (j) Matsumoto, T.; Gabbai, F. P. *Organometallics* **2009**, *28*, 4252–4253.
- (11) (a) Ueng, S. H.; Makhlof Brahmi, M.; Derat, E.; Fensterbank, L.; Lacôte, E.; Malacria, M.; Curran, D. P. *J. Am. Chem. Soc.* **2008**, *130*, 10082–10083. (b) Walton, J. C. *Angew. Chem., Int. Ed.* **2009**, *48*, 2–5. (c) The synthesis of **III** is described in ref 27.
- (12) (a) Ueng, S.-H.; Solov'yev, A.; Yuan, X.; Geib, S. J.; Fensterbank, L.; Lacôte, E.; Malacria, M.; Newcomb, M.; Walton, J. C.; Curran, D. P. *J. Am. Chem. Soc.* **2009**, *131*, 11256–11262. (b) Walton, J. C.; Makhlof Brahmi, M.; Fensterbank, L.; Lacôte, E.; Malacria, M.; Chu, Q.; Ueng, S. H.; Solov'yev, A.; Curran, D. P. *J. Am. Chem. Soc.* **2010**, DOI: 10.1021/ja909502q. (c) For another characterization of NHC-boryl radicals, see ref 10j.
- (13) (a) Rablen, P. R. *J. Am. Chem. Soc.* **1997**, *119*, 8350–8360. (b) Rablen, P. R.; Hartwig, J. F. *J. Am. Chem. Soc.* **1996**, *118*, 4648–4653.
- (14) (a) Walton, J. C.; McCarroll, A. J.; Chen, Q.; Carboni, B.; Nziengui, R. *J. Am. Chem. Soc.* **2000**, *122*, 5455–5463. (b) Carboni, B.; Monnier, L. *Tetrahedron* **1999**, *55*, 1197–1248.
- (15) Baban, J. A.; Roberts, B. P. *J. Chem. Soc., Perkin Trans. 2* **1988**, 1195–1200.
- (16) (a) Hahn, F. E.; Jahnke, M. *Angew. Chem., Int. Ed.* **2008**, *47*, 3122. (b) Marion, N.; Diez-Gonzalez, S.; Nolan, S. P. *Angew. Chem., Int. Ed.* **2007**, *46*, 2988. (c) Bourissou, D.; Guerret, O.; Gabbai, F. P.; Bertrand, G. *Chem. Rev.* **2000**, *100*, 39–92.
- (17) (a) Sheeller, B.; Ingold, K. U. *J. Chem. Soc., Perkin Trans. 2* **2001**, 480–486. (b) Lucarini, M.; Pedulli, G. F.; Valgimigli, L. *J. Org. Chem.* **1996**, *61*, 1161–1164.
- (18) (a) Lalevée, J.; Allonas, X.; Fouassier, J. P. *J. Am. Chem. Soc.* **2002**, *124*, 9613–9621. (b) Lalevée, J.; Graff, B.; Allonas, X.; Fouassier, J. P. *J. Phys. Chem. A* **2007**, *111*, 6991–6998.
- (19) Murov, S. L.; Carmichael, I.; Hug, G. L. *Handbook of Photochemistry*; Marcel Dekker: New York, 1993.
- (20) Rehm, D.; Weller, A. *Isr. J. Chem.* **1970**, *8*, 259–271.
- (21) (a) Frisch, M. J.; Trucks, G. W.; Schlegel, H. B.; Scuseria, G. E.; Robb, M. A.; Cheeseman, J. R.; Zakrzewski, V. G.; Montgomery, J. A., Jr.; Stratmann, R. E.; Burant, J. C.; Dapprich, S.; Millam, J. M.; Daniels, A. D.; Kudin, K. N.; Strain, M. C.; Farkas, O.; Tomasi, J.; Barone, V.; Cossi, M.; Cammi, R.; Mennucci, B.; Pomelli, C.; Adamo, C.; Clifford, S.; Ochterski, J.; Petersson, G. A.; Ayala, P. Y.; Cui, Q.; Morokuma, K.; Salvador, P.; Dannenberg, J. J.; Malick, D. K.; Rabuck, A. D.; Raghavachari, K.; Foresman, J. B.; Cioslowski, J.; Ortiz, J. V.; Baboul, A. G.; Stefanov, B. B.; Liu, G.; Liashenko, A.; Piskorz, P.; Komaromi, I.; Gomperts, R.; Martin, R. L.; Fox, D. J.; Keith, T.; Al-Laham, M. A.; Peng, C. Y.; Nanayakkara, A.; Challacombe, M.; Gill, P. M. W.; Johnson, B.; Chen, W.; Wong, M. W.; Andres, J. L.; Gonzalez, C.; Head-Gordon, M.; Replogle, E. S.; Pople, J. A. *Gaussian 03, Revision B-2*; Gaussian Inc.: Pittsburgh, PA, 2003. (b) Foresman, J. B.; Frisch, A. In *Exploring Chemistry with Electronic Structure Methods*, 2nd ed.; Gaussian Inc.: Pittsburgh, PA, 1996.
- (22) (a) Lalevée, J.; Allonas, X.; Jradi, S.; Fouassier, J. P. *Macromolecules* **2006**, *39*, 1872–1879. (b) Lalevée, J.; Zadoina, L.; Allonas, X.; Fouassier, J. P. *J. Polym. Sci., Part A: Chem.* **2007**, *45*, 2494–2502. (c) Lalevée, J.; El-Roz, M.; Allonas, X.; Fouassier, J. P. *J. Polym. Sci., Part A: Polym. Chem.* **2008**, *46*, 2008–2014.
- (23) El-Roz, M.; Lalevée, J.; Allonas, X.; Fouassier, J. P. *Macromolecules* **2009**, *42*, 8725–8732.
- (24) Bilevich, K. A.; Bubnov, N. N.; Ioffe, N. T.; Kalinkin, M. I.; Okhlobystin, O. Y.; Petrovskii, P. V. *Izv. Akad. Nauk SSSR, Ser. Khim.* **1971**, *8*, 1814–1815.
- (25) The TDDFT approach reproduced well the amine- and phosphine-boryl radicals spectra, too. See ref 7a.
- (26) Würtz, S.; Glorius, F. *Acc. Chem. Res.* **2008**, *41*, 1523–1533.
- (27) Similar spin delocalization has been calculated on slightly different structures. See: 12b.
- (28) (a) Crivello, J. V. In *Photoinitiators for Free Radical, Cationic and Anionic Photopolymerization*, 2nd ed.; Bradley, G., Ed.; New York, 1998. (b) Crivello, J. V. In *Ring-Opening Polymerization*; Brunelle, D. J., Ed.; Hanser: Munich, 1993. (c) Crivello, J. V.; Lam, J. H. W. *J. Polym. Sci., Polym. Chem. Ed.* **1979**, *17*, 1059–1065.
- (29) Lalevée, J.; Allonas, X.; Fouassier, J.-P. *Chem. Phys. Lett.* **2009**, *468*, 227–230.
- (30) A detailed analysis of the competition between hydrogen transfer and monomer quenching is presented for the <sup>3</sup>BP/silane system in ref 23.
- (31) Lalevée, J.; Allonas, X.; Fouassier, J.-P. *J. Phys. Chem. A* **2004**, *108*, 4326–4334.